PHYSICAL REVIEW E **113**, 045404 (2026)

Finite-time dehydration as a chemical reaction and its effect on counterion selectivity

I. Rubinstein,[1] M. Z. Bazant,[2] N. A. Kononenko,[3] V. V. Nikonenko,[3] and B. Zaltzman[4,*]
[1]*Blaustein Institutes for Desert Research, Ben-Gurion University of the Negev, Sede Boqer Campus, Israel*
[2]*Departments of Chemical Engineering and Mathematics, Massachusetts Institute of Technology, Cambridge, Massachusetts, USA*
[3]*Department of Physical Chemistry, Kuban State University, Krasnodar, Russia*
[4]*Department of Mathematics, Ben-Gurion University of the Negev, Beer-Sheva, Israel*

(Received 24 November 2025; accepted 11 March 2026; published 1 April 2026)

This paper contends that counterion dehydration at the ion-exchange membrane/electrolyte solution interface is an instance of heterogeneous reaction whose kinetics is governed by a rate equation of the Butler-Volmer type. The finite rate of this reaction is hypothesized to constitute an important factor that affects counterion selectivity of the membrane. Simple theoretical examples show that this is what may lead to the relatively easier membrane transfer of the less mobile ions (e.g., Li^+) compared to the more mobile ones (e.g., Na^+).

DOI: 10.1103/pvm2-bvmf

I. INTRODUCTION

Selectivity of ion-exchange membranes with respect to counterions of the same valency is an important feature of these membranes crucial for their use in ion separation processes. A preferable transfer of Li^+ ions compared to Na^+ and K^+ through the membrane is crucial for lithium recovery from ionic mixtures important for lithium-ion battery design. Heterogeneous and pseudohomogeneous ion-exchange membranes with a relatively high water content are hardly suitable for this purpose due to the presence of large-radius pores. The ratio between the mobilities of different counterions in such membranes is almost the same as in the solution, which does not allow for specific counterion-selective transfer [1–4]. However, when the water content is low, conductivity of the membrane may not correspond to the order of the counterion mobility in the solution. For example, the conductivity of Nafion 117 was found to decrease along the $Na^+ > Li^+ > K^+$ hierarchy, as opposed to $K^+ > Na^+ > Li^+$ for the bulk solution [5].

It is widely recognized that ion hydration is an important factor in controlling counterion selectivity [6–21]. This is taken into account in the design of various methods of lithium recovery from aqueous sources [22–25]. Recent years have seen the development of a fair number of Li-selective membranes. These are metal organic framework (MOF) membranes, crown-ether membranes, NASICON-type membranes made of crystalline materials, and graphene-based membranes [26–32]. All these membranes are characterized by subnanometer-sized aqueous regions ("pores") smaller than the size of a hydrated ion. Ion's dehydration at the membrane/solution interface and its contribution to counterion selectivity has been studied both experimentally and theoretically, including molecular dynamics simulations [15,30–34], and continuum modeling [8,15,28,35]. These studies showed that dehydration, partial or complete, at the interface between the solution and a nanopore or a nanopore membrane constitutes a significant factor affecting their ionic selectivity. In particular, it was concluded that preservation of one or several hydration shells is still compatible with the ionic transfer through the membrane [15,26,30,31,35–47].

Within a broader biophysical context, the importance of dehydration for selectivity of ionic channels, including the Na^+ and K^+ channels crucial in neural transport, has been commonly recognized [8,15,30,31,35–38,47–49]. It has been understood that ionic selectivity of these channels roots in a delicate interplay of the dehydration energy penalties and the permeating ions-channel-proteins interaction [27–43].

The purpose of this paper is to point out that a complete or partial interface dehydration is an instance of a slow local electric field driven heterogeneous reaction which is not a Faradaic reaction (no electron transfer involved). As such, it can still be modeled by the Butler-Volmer type of kinetic equation based on the classical picture of biasing the transition over a chemical barrier with a local electric field. Considering the length scale separation between the width of the diffusion layers and the membrane's thickness (typically tens-to-hundreds of micrometers) versus the width of the electric double layer (typically a few nanometers), the precise location of the reaction interface or its physical width are irrelevant in this context. The finite reaction rate may thus be a factor that affects selectivity, along with the difference of hydration and dehydration reaction rates related to the difference of the counterion hydration energies in the "solution" and "membrane" states. We illustrate this point by laying out simple examples in which a slower dehydration reaction rate of a more mobile ion (e.g., sodium) versus a faster reaction rate of a less mobile ion (e.g., lithium) yields selectivity of the membrane for the latter.

II. THE MODEL

Let us formulate the simplest dimensionless model of univalent cation transfer through a cation-selective membrane

---

[*] Contact author: boris@bgu.ac.il

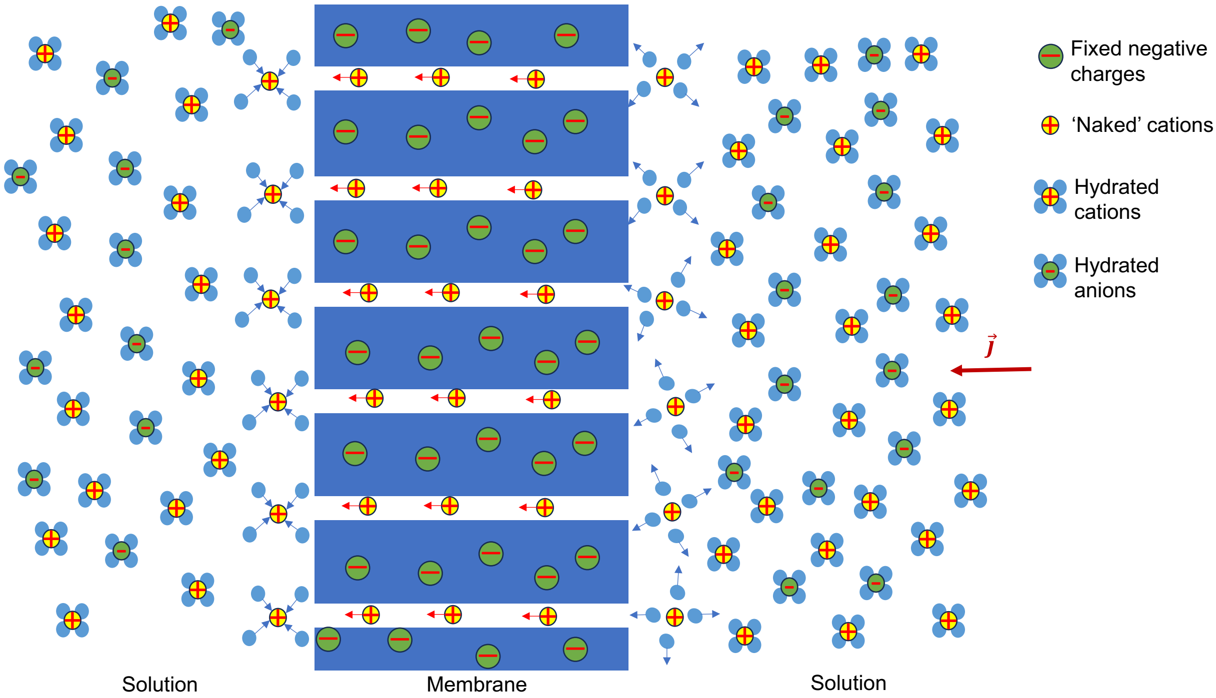

FIG. 1. Schematic representation of cation transfer through a subnanometer porous cation-selective membrane.

immersed in an electrolyte solution. We begin by considering a binary 1:1 valent electrolyte with specified concentration.

A. Binary electrolyte

We consider a perfectly perm-selective cation exchange membrane occupying the layer $0 < y < L$, where $y = \frac{\tilde{y}}{\tilde{l}}$, $\tilde{y}$ is the dimensional space variable, and $\tilde{l}$ is some characteristic length (e.g., 100 microns); see Fig. 1. Perfect cationic permselectivity of the membrane is modeled by postulating a vanishing anion flux along with equality of the dimensionless cation concentration in the membrane, $c = \frac{\tilde{c}}{\tilde{c}_0}$, to the constant membrane's fixed charge density, $N = \frac{\tilde{N}}{\tilde{c}_0}$. The variables with a tilde are the dimensional counterparts of the corresponding dimensionless variables; in particular, $\tilde{c}_0$ is the dimensional cation concentration in the bulk electrolyte solution. Thus, the dimensionless density of the electric current passing through the membrane reads

$$j = -DN\frac{d\varphi}{dy}, \tag{1}$$

where $j = \tilde{j}\frac{\tilde{l}}{\tilde{D}_0\tilde{c}_0}$, $\varphi = \frac{\tilde{\varphi}}{\tilde{\Phi}}$, and $\tilde{\Phi} = \frac{RT}{F}$. $D = \frac{\tilde{D}}{\tilde{D}_0}$ is the dimensionless cation diffusivity in the membrane and $\tilde{D}_0$ is the cation diffusivity in the solution.

Let us fix the dimensionless solution concentration at unity, which implies

$$c(0-) = c(L+) = 1. \tag{2}$$

Here, $y = 0-, y = L+$ correspond to the outer (solution) sides of the membrane/solution interface. Similarly, we prescribe the values of the electric potential as follows:

$$\varphi(0-) = -V, \varphi(L+) = 0, \tag{3}$$

where V is the dimensionless voltage drop across the membrane (including the Donnan interface jumps).

We complete the model formulation by imposing the Butler-Volmer-type kinetic equations [50,51] for the interface values of the dimensionless cation flux (electric current density being constant in the membrane):

$$-j = r_d e^{-\alpha\varphi(L)} - r_h N e^{(1-\alpha)\varphi(L)}, \tag{4a}$$

$$j = r_d e^{\alpha(-V-\varphi(0))} - r_h N e^{(1-\alpha)(V+\varphi(0))}. \tag{4b}$$

Here $r_h = \frac{\tilde{r}_h\tilde{l}}{\tilde{D}_0}$, $r_d = \frac{\tilde{r}_d\tilde{l}}{\tilde{D}_0}$ are the dimensionless hydration and dehydration reaction rates and α is the symmetry coefficient.

These equations are constructed so as to provide for continuity of the counterion electrochemical potential across the interface for infinite reaction rates.

Following the approach commonly used in electrochemistry, see [50,51], we address the equilibrium state, $j = 0$, and determine the equilibrium interface potential drop, $\delta\varphi$, as follows:

$$\delta\varphi = V_0 - \ln N. \tag{5}$$

Here V_0, $V_0 \overset{\text{def}}{=} \ln\frac{r_d}{r_h}$, is the dimensionless standard potential. In terms of the interface overpotentials, η_0, η_L, defined as

$$\eta_0 = \varphi(0) + V - \delta\varphi, \tag{6a}$$

$$\eta_L = \varphi(L) - \delta\varphi, \tag{6b}$$

Eq. (4) reads

$$-j = j_0(e^{-\alpha\eta_L} - e^{(1-\alpha)\eta_L}) = -j_0(e^{-\alpha\eta_0} - e^{(1-\alpha)\eta_0}), \tag{7}$$

where the factor j_0, reminiscent to the electrochemical exchange current density, is defined as follows:

$$j_0 \overset{\text{def}}{=} r_d^{1-\alpha}(r_h N)^\alpha. \tag{8}$$

Thus, the symmetry coefficients α and $1-\alpha$ are prescribing that fraction of the applied overpotential which is affecting the rate of dehydration α and hydration $1-\alpha$ reactions. In what follows we limit ourselves to the linear response that is to considering the low voltage regime:

$$-j = -j_0\eta_L = j_0\eta_0. \tag{9}$$

The integration of Eq. (1) yields

$$\eta_L - \eta_0 + V = -\frac{Lj}{DN}, \tag{10}$$

or, using (9),

$$\eta_0 = -\eta_L = \frac{1}{2}\left(V + \frac{Lj}{DN}\right). \tag{11}$$

Substitution of Eq. (11) into Eq. (9) yields the following flux/voltage relation valid for $\eta_0, \eta_L \ll 1$:

$$-j = j_0\eta_0 = \frac{j_0}{2}\left(V + \frac{Lj}{DN}\right) \tag{12}$$

and, therefore,

$$-j = \frac{V}{\frac{2}{j_0} + \frac{L}{DN}}. \tag{13}$$

This dependence implies that a less mobile ion with a higher hydration/dehydration rate may be transferred, preferably compared to a more mobile counterion with a slower hydration/dehydration. The relation (13) may be rewritten in terms of the effective membrane resistance R, $R \overset{\text{def}}{=} -\frac{V}{j}$, as follows:

$$R = \frac{2}{j_0} + \frac{L}{DN} = \frac{2e^{\alpha\delta\varphi}}{r_d} + \frac{L}{DN}. \tag{14}$$

Thus, for a fixed voltage, the cation flux depends on the counterion mobility in the membrane D and the exchange current j_0. Consequently, the system effective total resistance is a sum of the effective interfaces' resistances $\frac{2}{j_0}$ and the dimensionless membrane resistance $\frac{L}{DN}$. Through variation of the membrane width L or fixed charge density N (equivalent to variation of the solution concentration), the dependences (13), (14) may be used for direct experimental evaluation of j_0, that is of the hydration/dehydration reaction rate constant, $r_d^{1-\alpha}(r_h)^{\alpha}$. Thus, considering the high dilution limit in the relation (13), that is $N \gg 1$, yields a possibility of a direct experimental measurement of j_0 which is analogous to the measurement of the Taffel slope in electrochemistry. Next, in accordance with Eq. (8), assuming the symmetry coefficient equal one half $\alpha = \frac{1}{2}$, this yields the estimate for the typical dehydration/hydration rate constant as the geometric average of r_d and r_h.

The difference of hydration energies in the "solution" and "membrane" states may vary for different counterions. This variation yields not only difference of their respective equilibrium potential drops (5), (11), but also their different uptake by the membrane from the ionic mixture. This difference will express itself in an additional route to counterion selectivity which we illustrate for a ternary electrolyte (two different univalent counterions with the same univalent co-ion).

B. Ternary electrolyte

Below we generalize the previous model for a ternary 1:1:1 electrolyte with specified concentrations of two types of cations, $p^1 = \frac{\tilde{p}^1}{\tilde{c}_0}$, $p^2 = \frac{\tilde{p}^2}{\tilde{c}_0}$. Perfect cationic permselectivity of the membrane yields

$$p^1(y) + p^2(y) = N, 0 \leqslant y \leqslant L. \tag{15}$$

The dimensionless cation fluxes $j^i, i = 1, 2$, are constant in the membrane:

$$j^1 = -D^1\left(\frac{dp^1}{dy} - p^1\frac{d\varphi}{dy}\right), \tag{16a}$$

$$j^2 = -D^2\left(\frac{dp^2}{dy} - p^2\frac{d\varphi}{dy}\right). \tag{16b}$$

Here, D^i, $i = 1, 2$ are the dimensionless cation diffusivities in the membrane. Equations (15) and (16) yield the constancy of the dimensionless electric field in the membrane:

$$-\frac{d\varphi}{dy} = \frac{1}{N}\left(\frac{j^1}{D^1} + \frac{j^2}{D^2}\right). \tag{17}$$

The boundary conditions are similar to those applied for the binary electrolyte case. We assume equal solution concentration of cations of both kinds fixing them at unity

$$\varphi(0-) = -V, \quad \varphi(L+) = 0. \tag{18}$$

We complete the formulation by imposing once more the Butler-Volmer-type kinetic equations [50,51] for the interface values of the dimensionless cation fluxes:

$$-j^1 = r_d^1 e^{-\alpha\varphi(L)} - r_h^1 p^1(L)e^{(1-\alpha)\varphi(L)}, \tag{19a}$$

$$-j^2 = r_d^2 e^{-\alpha\varphi(L)} - r_h^2 p^2(L)e^{(1-\alpha)\varphi(L)}, \tag{19b}$$

$$j^1 = r_d^1 e^{\alpha(-V-\varphi(0))} - r_h^1 p^1(0)e^{(1-\alpha)(V+\varphi(0))}, \tag{19c}$$

$$j^2 = r_d^2 e^{\alpha(-V-\varphi(0))} - r_h^2 p^2(0)e^{(1-\alpha)(V+\varphi(0))}. \tag{19d}$$

Here, $r_h^i = \frac{\tilde{r}_h\tilde{l}}{\tilde{D}_0}$, $r_d^i = \frac{\tilde{r}_d\tilde{l}}{\tilde{D}_0}$, $i = 1, 2$ are the dimensionless hydration and dehydration reaction rate constants for each type of cation, and the symmetry factor α is assumed to be the same for the cations of both types. Following [50,51], we address the equilibrium state, $j^i = 0$, and determine the equilibrium interface potential drop, $\delta\varphi$, and equilibrium interface cation concentrations, $\mathbf{P}^1$ and $\mathbf{P}^2$, as follows:

$$\delta\varphi = \ln\frac{e^{V_1} + e^{V_2}}{N}, \tag{20a}$$

$$\mathbf{P}^1 = e^{V_1-\delta\varphi}, \tag{20b}$$

$$\mathbf{P}^2 = e^{V_2-\delta\varphi}. \tag{20c}$$

Here, $V_i = \ln\frac{r_d^i}{r_h^i}$, $i = 1, 2$ are the respective interface increments of the counterionic standard potentials.

In terms of the interface overpotentials η_0, η_L, defined by ([6]) Eq. (19), read

$$-j^1 = j_0^1\left(e^{-\alpha\eta_L} - \frac{p^1(L)}{\mathbf{P}^1}e^{(1-\alpha)\eta_L}\right), \tag{21a}$$

$$-j^2 = j_0^2\left(e^{-\alpha\eta_L} - \frac{p^2(L)}{\mathbf{P}^2}e^{(1-\alpha)\eta_L}\right), \tag{21b}$$

$$j^1 = j_0^1\left(e^{-\alpha\eta_0} - \frac{p^1(L)}{\mathbf{P}^1}e^{(1-\alpha)\eta_0}\right), \tag{21c}$$

$$j^2 = j_0^2\left(e^{-\alpha\eta_0} - \frac{p^2(L)}{\mathbf{P}^2}e^{(1-\alpha)\eta_0}\right), \tag{21d}$$

where the factors j_0^1, j_0^2 are defined as follows:

$$j_0^1 = \left(r_d^1\right)^{1-\alpha}\left(r_h^1\mathbf{P}^1\right)^{\alpha} = r_d^1 e^{-\alpha\delta\varphi}, \tag{22a}$$

$$j_0^2 = \left(r_d^2\right)^{1-\alpha}\left(r_h^2\mathbf{P}^2\right)^{\alpha} = r_d^2 e^{-\alpha\delta\varphi}. \tag{22b}$$

Similarly to the binary electrolyte case we limit ourselves by addressing the low voltage regime. In this case, $|j^1| \ll 1, |j^2| \ll 1, |\eta_0| \ll 1, |\eta_L| \ll 1, |\delta p^1| \ll 1, |\delta p^2| \ll 1$. Here, $|\delta p^1|$ and $|\delta p^2|$ are the deviations of the corresponding cation concentrations from their equilibrium values: $\delta p^1 \overset{\text{def}}{=} p^1 - \mathbf{P}^1$, $\delta p^2 \overset{\text{def}}{=} p^2 - \mathbf{P}^2$. Then, keeping the leading order terms in Eq. (21) (thus, limiting ourselves to the linear response), we obtain

$$-\frac{j^1}{j_0^1}\mathbf{P}^1 = -\mathbf{P}^1\eta_L - \delta p^1(L), \tag{23a}$$

$$-\frac{j^2}{j_0^2}\mathbf{P}^2 = -\mathbf{P}^2\eta_L - \delta p^2(L), \tag{23b}$$

$$\frac{j^1}{j_0^1}\mathbf{P}^1 = -\mathbf{P}^1\eta_0 - \delta p^1(0), \tag{23c}$$

$$\frac{j^2}{j_0^2}\mathbf{P}^2 = -\mathbf{P}^2\eta_0 - \delta p^2(0). \tag{23d}$$

Summing Eqs. (23a) and (23b), and Eqs. (23c) and (23d), we find that

$$\eta_0 = -\eta_L. \tag{24}$$

To evaluate the effect of concentration polarization in the membrane, that is the transmembrane variation of δp^1, δp^2, we substitute Eq. (23) into Eq. (16) and integrate the resulting equations. Keeping the leading order terms in the obtained equations, we obtain

$$\begin{aligned}\delta p^1(L) - \delta p^1(0) &= -(\delta p^2(L) - \delta p^2(0))\\ &= \left(\mathbf{P}^1\frac{j^2}{ND^2} - \mathbf{P}^2\frac{j^1}{ND^1}\right).\end{aligned} \tag{25}$$

Substituting Eq. (25) into Eq. (23) and taking into account Eq. (24), we find that

$$2\frac{j^1}{j_0^1}\mathbf{P}^1 = -2\eta_0 + \left(\frac{j^2}{ND^2} - \frac{\mathbf{P}^2}{\mathbf{P}^1}\frac{j^1}{ND^1}\right)L, \tag{26a}$$

$$2\frac{j^2}{j_0^2}\mathbf{P}^1 = -2\eta_0 + \left(\frac{j^1}{ND^1} - \frac{\mathbf{P}^1}{\mathbf{P}^2}\frac{j^2}{ND^2}\right)L, \tag{26b}$$

and, therefore,

$$\frac{j^2}{j^1} = \frac{\sigma^2}{L^2} : \frac{\sigma^1}{L^1}. \tag{27}$$

Here, σ^i and L^i, $i = 1, 2$ are, respectively, the partial equilibrium ionic conductivities, that is the contributions of particular counterions to the equilibrium membrane conductivity, and the effective membrane widths defined as follows:

$$\sigma^i \overset{\text{def}}{=} D^i\mathbf{P}^i, \tag{28a}$$

$$L^i \overset{\text{def}}{=} 2e^{\alpha\delta\varphi}\frac{\sigma^i}{r_d^i} + L. \tag{28b}$$

To complete this analysis, we integrate Eq. (17) and obtain the following relation between the overpotentials and the cation fluxes:

$$\eta_L = -\eta_0 = -\frac{1}{2}\left(V + \frac{L}{N}\left(\frac{j^1}{D^1} + \frac{j^2}{D^2}\right)\right). \tag{29}$$

Substituting Eq. (29) into Eq. (26) we obtain the following voltage/fluxes relations:

$$j^1 = -V\frac{\sigma^1}{L^1}, \tag{30a}$$

$$j^2 = -V\frac{\sigma^2}{L^2}. \tag{30b}$$

In terms of the partial effective ionic resistances, $R^i \overset{\text{def}}{=} -\frac{V}{j^i}$, $i = 1, 2$, the relation (30) reads

$$R^1 = \frac{L^1}{\sigma^1} = \frac{2e^{\alpha\delta\varphi}}{r_d^1} + \frac{L}{D^1\mathbf{P}^1}, \tag{31a}$$

$$R^2 = \frac{L^2}{\sigma^2} = \frac{2e^{\alpha\delta\varphi}}{r_d^2} + \frac{L}{D^2\mathbf{P}^2}. \tag{31b}$$

Expression (31) shows the direct ternary mixture analogs of expression (14) valid for the binary solution.

III. CONCLUSIONS

Our analysis of the binary case suggests that it is well suited for the experimental evaluation of the ionic hydration/dehydration reaction rate constants. Our conclusions from the ternary case analysis may be summarized as follows.

For a fixed voltage, the cation fluxes depend on the partial equilibrium ionic conductivities σ^i, and on the effective membrane widths L^i. This dependence implies that a less mobile ion with a higher dehydration rate may be transferred preferably compared to a more mobile counterion with slower dehydration. On the other hand, the equilibrium counterion concentrations in the membrane depend on the difference of hydration energies in the "solution" and "membrane" states which may be different for different counterions. This difference may be another source of the membrane counterion selectivity which is best understood in the limit of infinite hydration/dehydration reaction rate resulting in the interface equilibrium. In this case, different interface drops of hydration energies for different counterions will simply result in different coefficients of their distribution between the solution and the membrane that is their partial equilibrium conductivities. For equal other factors, this will result in the preferred transfer of the counterion, preferably up taken by the membrane.

We illustrate these conclusions first by plotting in Fig. 2 the logarithmic membrane selectivity $\mu \overset{\text{def}}{=} \ln\frac{j^2}{j^1}$ as a function of the partial equilibrium ionic conductivities ratio $\rho \overset{\text{def}}{=} \frac{\sigma^1}{\sigma^2}$ and the effective length ratio $\lambda \overset{\text{def}}{=} \frac{L^2}{L^1}$, where positive

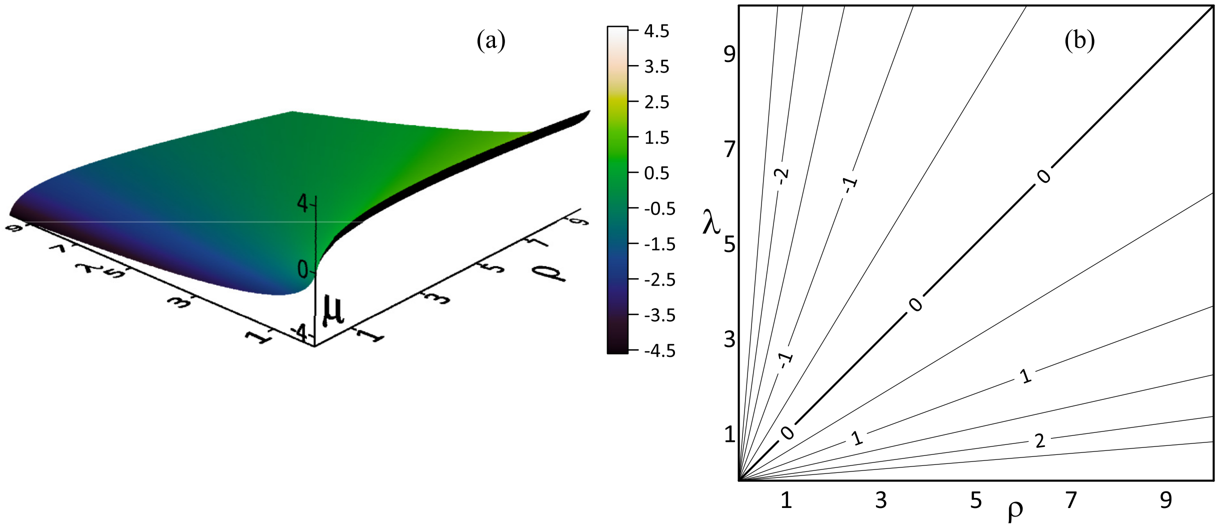

FIG. 2. Membrane selectivity μ vs partial equilibrium ionic conductivities ratio $\rho = \frac{\sigma^1}{\sigma^2}$, and the effective width ratio $\lambda = \frac{L^2}{L^1}$. 3D plot (a) and μ-level lines (b).

μ corresponds to the membrane selective to the ions of the second kind and its negative values correspond to the membrane selective to the ions of the first kind.

Second, for illustration, we consider the following limiting modes: (i) Thin membrane $L \ll 1$ (equivalently, high dilution limit $N \gg 1$), (ii) thick membrane, $L \gg 1$, c) Infinite reaction rate limit, $r_d^i, r_h^i \gg 1$, $\frac{r_d^i}{r_h^i} = O(1)$, $i = 1, 2$.

(i) For a thin membrane $L \ll 1$, the effective membrane width is mediated by the partial ionic conductivity/reaction rate ratio $L^i = 2e^{\alpha\delta\varphi}\frac{\sigma^i}{r_d^i}$, $i = 1, 2$, and, accordingly, the partial effective ionic resistances are mediated by their interface contributions $R^i = 2\frac{e^{\alpha\delta\varphi}}{r_d^i}$, $i = 1, 2$. Therefore,

$$j^1 = -V\frac{e^{-\alpha\delta\varphi}}{2}r_d^1, \tag{32a}$$

$$j^2 = -V\frac{e^{-\alpha\delta\varphi}}{2}r_d^2, \tag{32b}$$

and, thus,

$$\frac{j^2}{j^1} = \frac{r_d^2}{r_d^1}. \tag{33}$$

Thus, for a thin membrane, the counterion selectivity is solely determined by the interplay of the counterions' dehydration rates. Equation (33) complements the path to experimental evaluation of the average dehydration/hydration rate constants suggested in Sec. II A, with a possibility of experimentally testing the dehydration rate effect upon the membrane counterion selectivity.

(ii) For a thick membrane $L \gg 1$, the effective membrane width equals the physical membrane width $L^i = L$ and the partial effective ionic resistances are mediated by their transmembrane contributions $R^i = \frac{L}{D^i\mathbf{P}^i}$, $i = 1, 2$. Therefore,

$$j^1 = -V\frac{\sigma^1}{L}, \tag{34a}$$

$$j^2 = -V\frac{\sigma^2}{L}, \tag{34b}$$

and, thus,

$$\frac{j^2}{j^1} = \frac{\sigma^2}{\sigma^1}. \tag{35}$$

(iii) Relations (34) and (35) also hold for the infinite reaction rate limit, $r_d^i, r_h^i \gg 1$, $\frac{r_d^i}{r_h^i} = O(1)$, $i = 1, 2$.

ACKNOWLEDGMENTS

We thank Dr. Tatiana Philippova for thoroughly proofreading and editing the manuscript. This work was supported by the Israel Science Foundation (ISF) under Grant No. 547/23.

DATA AVAILABILITY

No data were created or analyzed in this study.

---

[1] N. P. Berezina, N. A. Kononenko, O. A. Dyomina, and N. P. Gnusin, Characterization of ion-exchange membrane materials: properties vs structure, Adv. Colloid Interface Sci. **139**, 3 (2008).

[2] L. V. Karpenko-Jereb and N. P. Berezina, Determination of structural, selective, electrokinetic and percolation characteristics of ion-exchange membranes from conductive data, Desalination **245**, 587 (2009).

[3] R. Epsztein, E. Shaulsky, M. Qin, and M. Elimelech, Activation behavior for ion permeation in ion-exchange membranes: Role of ion dehydration in selective transport, J. Membr. Sci. **580**, 316 (2019).

[4] V. I. Volkov, A. V. Chernyak, D. V. Golubenko, V. A. Tverskoy, G. A. Lochin, E. S. Odjigaeva, and A. B. Yaroslavtsev, Hydration and diffusion of H$^+$, Li$^+$, Na$^+$, Cs$^+$ ions in cation-exchange, membranes based on Polyethylene- and

sulfonated-grafted polystyrene studied by NMR technique and ionic conductivity measurements, Membranes **10**, 272 (2020).

[5] I. A. Stenina, Ph. Sistat, A. I. Rebrov, G. Pourcelly, and A. B. Yaroslavtsev, Ion mobility in Nafion-117 membranes, Desalination **170**, 49 (2004).

[6] J. R. Bontha and P. N. Pintauro, Water orientation and ion solvation effects during multicomponent salt partitioning in a Nafion cation exchange membrane, Chem. Eng. Sci. **49**, 3835 (1994).

[7] R. Epsztein, E. Shaulsky, N. Dizge, D. M. Warsinger, and M. Elimelech, Role of ionic charge density in donnan exclusion of monovalent anions by nanofiltration, Environ. Sci. Technol. **52**, 4108 (2018).

[8] X. Zhou, Zh Wang, R. Epsztein, Ch. Zhan, W. Li, J. D. Fortner, T. A. Pham, J. H. Kim, and M. Elimelech, Intrapore energy barriers govern ion transport and selectivity of desalination membranes, Sci. Adv. **6**, eabd9045 (2020).

[9] V. Pavluchkov, I. Shefer, O. Peer-Haim, J. Blotevogel, and R. Epsztein, Indications of ion dehydration in diffusion-only and pressure-driven nanofiltration, J. Membr. Sci. **648**, 120358 (2022).

[10] L. Baudino, C. Santos, C. F. Pirri, F. La Mantia, and A. Lamberti, Recent advances in the lithium recovery from water resources: From passive to electrochemical methods, Adv. Sci. **9**, 2201380 (2022).

[11] V. I. Volkov, N. A. Slesarenko, A. V. Chernyak, I. A. Avilova, and V. P. Tarasov, Hydration and mobility of alkaline metal cations in sulfonic cation exchange membranes, Membranes **13**, 518 (2023).

[12] T. Kanagasundaram, O. Murphy, M. N. Haji, and J. J. Wilson, The recovery and separation of lithium by using solvent extraction methods, Coord. Chem. Rev. **509**, 215727 (2024).

[13] D. Yu Butylskii, V. A. Troitskiy, N. V. Smirnova, N. D. Pismenskaya, Y. Wang, C. Jiang, T. Xu, and V. V. Nikonenko, Review of recent progress on lithium recovery and recycling from primary and secondary sources with membrane-based technologies, Desalination **586**, 117826 (2024).

[14] Z. H. Foo and J. H. Lienhard, Emerging membrane technologies for sustainable lithium extraction from brines and leachates: Innovations, challenges, and industrial scalability, Desalination **598**, 118411 (2025).

[15] A. Ershov, H. Xu, Y. Li, T. Tong, and R. Epsztein, Role of ion dehydration in ion-ion selectivity of dense membranes, Environ. Sci. Technol. **59**, 17997 (2025).

[16] T. Jain, B. C. Rasera, R. J. S. Guerrero, M. S. H. Boutilier, S. C. O'Hern, J.-C. Idrobo, and R. Karnik, Heterogeneous sub-continuum ionic transport in statistically isolated graphene nanopores, Nat. Nanotechnol. **10**, 1053 (2015).

[17] L. A. Richards, A. I. Schäfer, B. S. Richards, and B. Corry, The importance of dehydration in determining ion transport in narrow pores, Small **8**, 1701 (2012).

[18] C. Lu, C. Hu, C. L. Ritt, X. Hua, J. Sun, H. Xia, Y. Liu, D. W. Li, B. Ma, M. Elimelech, and J. Qu, *In situ* characterization of dehydration during ion transport in polymeric nanochannels, J. Am. Chem. Soc. **143**, 14242 (2021).

[19] R. Epsztein, R. M. DuChanois, C. L. Ritt, A. Noy, and M. Elimelech, Towards single species selectivity of membranes with subnanometre pores, Nat. Nanotechnol. **15**, 426 (2020).

[20] H. B. Park, J. Kamcev, L. M. Robeson, M. Elimelech, and B. D. Freeman, Maximizing the right stuff: the trade-off between membrane permeability and selectivity, Science **356**, eaab0530 (2017).

[21] K. Liu, R. Epsztein, Sh. Lin, L. Liu, J. Qu, and M. Sun, Electrostatic-driven dehydration of ions in nanoporous membranes, Sci. Adv. **11**, eadv0174 (2025).

[22] H. Zhang, J. Hou, Y. Hu, P. Wang, R. Ou, L. Jiang, J. Zhe Liu, B. D. Freeman, A. J. Hill, and H. Wang, Ultrafast selective transport of alkali metal ions in metal organic frameworks with subnanometer pores, Sci. Adv. **4**, eaaq0066 (2018).

[23] S. J. Warnock, R. Sujananib, E. S. Zofchakb, S. Zhaoc, T. J. Dilenschneiderb, K. G. Hansonc, S. Mukherjeed, V. Ganesanb, B. D. Freemanb, M. M. Abu-Omarc, and C. M. Batesa, Engineering Li/Na selectivity in 12-Crown-4-functionalized polymer membranes, Proc. Natl. Acad. Sci. USA **118**, e2022197118 (2021).

[24] X. Yin, P. Xu, and H. Wang, Modification of cation exchange membranes for enhanced extraction of lithium from magnesium and sodium brine solutions via selective electrodialysis, J. Membr. Sci. **701**, 122705 (2024).

[25] F. Fan, Y. Ren, S. Zhang, Z. Tang, J. Wang, X. Han, Y. Yang, G. Lu, Y. Zhang, L. Chen, Z. Wang, K. Zhang, J. Gao, J. Zhao, G. Cui, and B. Tang, A bioinspired membrane with ultrahigh Li^+/Na^+ and Li^+/K^+ separations enables direct lithium extraction from brine, Adv. Sci. **11**, 2402898 (2024).

[26] S. Sahu, M. D. Ventra, and M. Zwolak, Dehydration as a universal mechanism for ion selectivity in graphene and other atomically thin pores, Nano Lett. **17**, 4719 (2017).

[27] E. S. Zofchak, Z. Zhang, B. K. Wheatle, R. Sujanani, S. J. Warnock, T. J. Dilenschneider, K. G. Hanson, Sh. Zhao, S. Mukherjee, M. M. Abu-Omar, Chr. M. Bates, B. D. Freeman, and V. Ganesan, Origins of lithium/sodium reverse permeability selectivity in 12-Crown-4-functionalized polymer membranes, ACS Macro Lett. **10**, 1167 (2021).

[28] R. S. Kingsbury, M. A. Baird, J. Zhang, H. D. Patel, M. J. Baran, B. A. Helms, and E. M. V. Hoek, Kinetic barrier networks reveal rate limitations in ion-selective membranes, Matter **7**, 2161 (2024).

[29] K. Liu, R. Epsztein, S. Lin, J. Qu, and M. Sun, Ion–ion selectivity of synthetic membranes with confined nanostructures, ACS Nano **18**, 21633 (2024).

[30] B. Corry, The naked truth about K selectivity, Nat. Chem. **10**, 799 (2018).

[31] W. Kopec, D. A. Köpfer, O. N. Vickery, A. S. Bondarenko, T. L. C. Jansen, B. L. de Groot, and U. Zachariae, Direct knock-on of desolvated ions governs strict ion selectivity in K channels, Nat. Chem. **10**, 813 (2018).

[32] T. Xu, B. Wu, W. Li, Y. Li, Y. Zhu, F. Sheng, Q. Li, L. Ge, X. Li, H. Wang, and T. Xu, Perfect confinement of crown ethers in MOF membrane for complete dehydration and fast transport of monovalent ions, Sci. Adv. **10**, eadn0944 (2024).

[33] C. L. Ritt, M. Liu, T. A. Pham, R. Epsztein, H. J. Kulik, and M. Elimelech, Machine learning reveals key ion selectivity mechanisms in polymeric membranes with subnanometer pores, Sci. Adv. **8**, eabl5771 (2022).

[34] F. Liu and D. Sun, Ion distribution and hydration structure at solid–liquid interface between NaCl crystal and its solution, ACS Omega **4**, 18692 (2019).

[35] N. R. Latorraca, K. M. Callenberg, J. P. Boyle, and M. Grabe, Continuum approaches to understanding ion and peptide interactions with the membrane, J. Membr. Biol. **247**, 395 (2014).

[36] S. W. Lockless, M. Zhou, and R. MacKinnon, Structural and thermodynamic properties of selective ion binding in a K^+ Channel, PLoS Biol. **5**, e121 (2007).

[37] H. T. Kratochvil, J. K. Carr, K. Matulef, A. W. Annen, H. Li, M. Maj, J. Ostmeyer, A. L. Serrano, H. Raghuraman, S. D. Moran, J. L. Skinner, E. Perozo, B. Roux, F. I. Valiyaveetil, and M. T. Zanni, Instantaneous ion configurations in the K^+ ion channel selectivity filter revealed by 2D IR spectroscopy, Science **353**, 1040 (2016).

[38] B. Roux, Ion channels and ion selectivity, Essays Biochem. **61**, 201 (2017).

[39] M. L. Barabash, W. A. T. Gibby, C. Guardiani, A. Smolyanitsky, D. G. Luchinsky, and P. V. E. McClintock, Origin and control of ionic hydration patterns in nanopores, Commun. Mater. **2**, 65 (2021).

[40] C. Song and B. Corry, Intrinsic ion selectivity of narrow hydrophobic pores, J. Phys. Chem. B **113**, 7642 (2009).

[41] H. Li, J. S. Francisco, and X. C. Zeng, Unraveling the mechanism of selective ion transport in hydrophobic subnanometer channels, Proc. Natl. Acad. Sci. USA **112**, 10851 (2015).

[42] Y. Li, Y. Yu, J. Qian, H. Wu, and F. Wang, Anomalous ion transport through angstrom-scale pores: Effect of hydration shell exchange on ion mobility, Appl. Surf. Sci. **560**, 150022 (2021).

[43] M. Wang, W. Shen, S. Ding, X. Wang, Z. Wang, Y. Wang, and F. Liu, A coupled effect of dehydration and electrostatic interactions on selective ion transport through charged nanochannels, Nanoscale **10**, 18821 (2018).

[44] C. Lu, C. Hu, Z. Chen, P. Wang, F. Feng, G. He, F. Wang, Y. Zhang, J. Zh Liu, X. Zhang, and J. Qu, Dehydration-enhanced ion-pore interactions dominate anion transport and selectivity in nanochannels, Sci. Adv. **9**, eadf8412 (2023).

[45] H. Bhatti, Y.-L. Ying, and Y.-T. Long, How to compare the ion selectivity of smart nanopores/membranes, Research **7**, 0506 (2024).

[46] C. Park, P. A. Fenter, K. L. Nagy, and N. C. Sturchio, Hydration and distribution of ions at the mica-water interface, Phys. Rev. Lett. **97**, 016101 (2006).

[47] S. Y. Noskov and B. Roux, Importance of hydration and dynamics on the selectivity of the KcsA and NaK channels, J. Gen. Physiol. **129**, 135 (2007).

[48] S. Oh, F. Marinelli, W. Zhou, J. Lee, H. J. Choi, M. Kim, J. D Faraldo-Gómez, and R. K Hite, Differential ion dehydration energetics explains selectivity in the non-canonical lysosomal K^+ channel TMEM175, eLife **11**, e75122 (2022).

[49] J. J. Finnerty, A. Peyser, and P. Carloni, Cation selectivity in biological cation channels using experimental structural information and statistical mechanical simulation, PLoS ONE **10**, e0138679 (2015).

[50] M. Z. Bazant, K. T. Chu, and B. J. Bayly, Current-voltage relations for electrochemical thin films, SIAM J. Appl. Math. **65**, 1463 (2005).

[51] M. Z. Bazant, Unified quantum theory of electrochemical kinetics by coupled ion-electron transfer, Faraday Discuss. **246**, 60 (2023).